Title

A method for monitoring enamel erosion using laser irradiated surfaces and optical coherence tomography

Journal

Lasers in Surgery and Medicine, 46(9)

ISSN

1050-9267

Authors

Chan, Kenneth H
Tom, Henry
Darling, Cynthia L
et al.

Publication Date

2014-11-01

DOI

10.1002/lsm.22285

Peer reviewed

HHS Public Access

Author manuscript

Lasers Surg Med. Author manuscript; available in PMC 2015 December 10.

Published in final edited form as:

Lasers Surg Med. 2014 November ; 46(9): 672–678. doi:10.1002/lsm.22285.

A Method for Monitoring Enamel Erosion Using Laser Irradiated Surfaces and Optical Coherence Tomography

Kenneth H. Chan, **Henry Tom**, **Cynthia L. Darling, PhD**, and **Daniel Fried, PhD***

University of California, San Francisco, San Francisco, California 94143-0758

Abstract

Introduction—Since optical coherence tomography (OCT) is well suited for measuring small dimensional changes on tooth surfaces, OCT has great potential for monitoring tooth erosion. Previous studies have shown that enamel areas ablated by a carbon dioxide laser manifested lower rates of erosion compared to the non-ablated areas. The purpose of this study was to develop a model to monitor erosion *in vitro* that could potentially be used *in vivo.*

Methods—Thirteen bovine enamel blocks were used in this *in vitro* study. Each 10 mm × 2 mm block was partitioned into five regions, the central region was unprotected, the adjacent windows were irradiated by a CO_2 laser operating at 9.3 μm with a fluence of 2.4J/cm^2, and the outermost windows were coated with acid resistant varnish. The samples were exposed to a pH cycling regimen that caused both erosion and subsurface demineralization for 2, 4 and 6 days. The surfaces were scanned using a time-domain polarization sensitive optical coherence tomography (PS-OCT) system and the degree of surface loss (erosion) and the integrated reflectivity with lesion depth was calculated for each window.

Results—There was a large and significant reduction in the depth of surface loss (erosion) and the severity of demineralization in the areas irradiated by the laser.

Conclusion—Irradiation of the enamel surface with a pulsed carbon dioxide laser at sub-ablative intensities results in significant inhibition of erosion and demineralization under the acid challenge employed in this study. In addition, these results suggest that it may be feasible to modify regions of the enamel surface using the laser to serve as reference marks to monitor the rate of erosion *in vivo*.

Keywords

tooth erosion; tooth demineralization; carbon dioxide laser; optical coherence tomography

INTRODUCTION

Dental erosion consists of the removal and softening of tooth surfaces and it is often accompanied by subsurface dissolution of the mineral. It is a multifactorial condition with

*Corresponding Author: Daniel Fried, Ph.D, Department of Preventive and Restorative Dental Sciences, University of California, San Francisco, San Francisco 707 Parnassus Ave. 94143, daniel.fried@ucsf.edu.

Conflict of Interest Disclosures: All authors have completed and submitted the ICMJE Form for Disclosure of Potential Conflicts of Interest and none were reported.

both chemical and mechanical contributions and it is an increasing problem with the widespread consumption of soft drinks [1]. Early detection and diagnosis is important and there are currently no devices available for the specific detection of dental erosion in clinical practice [2]. Optical coherence tomography is capable of measuring dimensional changes nondestructively on tooth surfaces in addition to the subsurface demineralization.

Previous studies have shown that polarization sensitive optical coherence tomography (PS-OCT) can nondestructively measure the severity of subsurface demineralization in enamel and dentin and is therefore well suited for this role [3–14]. Early *in vitro* studies of the use of OCT for monitoring tooth demineralization demonstrated that OCT can be used to measure the loss of enamel due to exposure to a demineralizing solution. In the study of Fried et al. [7], acid resistant varnish was added to a control surface and this surface served as a reference surface to quantify the loss of enamel exposed to erosion. Although this approach is simple to implement *in vitro*, more robust adhesives such as composites would be needed in order to employ it *in vivo* and they would have to be employed in areas that are not subject to wear.

Studies have also employed OCT to monitor the remaining enamel thickness by using the dentinal enamel junction (DEJ) as a reference [15]. However, there are many challenges in accurately measuring the remaining enamel thickness. The structure of the DEJ can be described as scalloped with its convexities directed toward the dentine and concavities toward the enamel, therefore it does not present a sharp boundary. Moreover, dispersion of the light after passage through enamel causes decreased resolution. If erosion is accompanied by subsurface demineralization or roughening of the surface, the strong increase in light scattering interferes with the ability to accurately resolve the DEJ [16]. Moreover, the tooth surface is often covered by a layer of saliva, which causes additional variation in the optical path length [16].

One can also achieve the inhibition of demineralization and erosion via laser irradiation [17–19]. We discovered that the area of enamel surrounding the laser irradiated reference incisions used to separate our sample windows (see Fig. 1) manifested increased resistance to erosion. Under a highly erosive acid challenge the laser irradiated areas were preferentially protected and not eroded, and these areas protruded above the surrounding eroded untreated enamel erosion areas [20]. Last year, we carried out further studies exploiting the enhanced resistance to erosion of laser treated surfaces to assess the suitability of using it as a method to quantify the rate of erosion and found that the laser-ablated areas appeared quite effective in inhibiting the surface loss in a demineralization model [16]. We recently presented a conference paper showing that sub-ablative fluences can be effective as well [21].

The purpose of this study was to develop an *in vitro* model to monitor erosion with OCT that can potentially be translated to an *in vivo* setting, utilizing sub-ablative laser irradiation intensities.

MATERIALS AND METHODS

Sample Preparation and Erosion Model

Thirteen bovine enamel blocks, approximately 8–12 mm in length, 2 mm in width, and a thickness of ~1 mm of bovine enamel were prepared from extracted tooth incisors acquired from a slaughterhouse. Each enamel sample was partitioned into five regions or windows (two sound, two laser irradiated, and one unprotected) by etching 140 μm wide incisions 2 mm apart across each of the enamel blocks (see Fig. 1). Incisions were etched using a transverse excited atmospheric pressure (TEA) CO_2 laser operating at 9.3 μm with a fluence of 200J/cm^2, Impact 2500, GSI Lumonics (Rugby, U.K.). In the windows adjacent to the center, a sub-ablative incident fluence of 2.4J/cm^2 was used. The sub-ablative fluence was used to increase resistance to acid dissolution, protecting the region from further demineralization and erosion. In the outer most windows, a thin layer of acid resistant varnish, red nail polish, Revlon (New York, NY) was applied to protect the sound enamel control area. The center window was left unprotected.

All samples were exposed to a pH cycling model with a demineralization solution composed of a 40 ml aliquot of 2.0 mmol/L calcium, 2.0 mmol/L phosphate, and a 0.075 mol/L acetate at pH 4.5 followed up with remineralization solution comprised of a 40 ml aliquot of 1.5 mmol/L calcium, 0.9 mmol/L phosphate, 150 mmol/L potassium choloride, and 20 mmol/L HEPES at pH 7.0. Each of the cycles was repeated twice (2, 4, 6 cycles) for the central three windows. Thirteen blocks were exposed to a daily pH cycling regimen consisting of immersion in a demineralization solution (pH 4.5) for 6 h, followed by a rinse with deionized water, and immersion in a remineralization solution (pH 7.0) for 17 h at 37°C. After every 2 days or cycles, PS-OCT scans were taken to assess the amount of erosion that had taken place by comparing the heights of the demineralized window and sub-ablative regions to that of the protected ends of the sample. After the last day of pH cycling (Day-6), the acid resistant varnish was removed with acetone.

PS-OCT System

An all-fiber-based optical coherence domain reflectometry (OCDR) system (time-domain) with polarization maintaining (PM) optical fiber, high-speed piezoelectric fiber-stretchers and two balanced InGaAs receivers that was designed and fabricated by Optiphase, Inc., (Van Nuys, CA) was used. This two-channel system was integrated with a broadband superluminescent diode (SLD) Denselight (Jessup, MD) and a high-speed XY-scanning system (ESP 300 controller and 850G-HS stages, Newport, Irvine, CA) for *in vitro* optical coherence tomography. This system is based on a polarization-sensitive Michelson interferometer. Thehighpower (15mW) polarized SLD sourceoperated at a center wavelength of 1317nm with a spectral bandwidth full-width at half-maximum (FWHM) of 84nm. The sample arm was coupled to an AR-coated fiber-collimator to produce a 6 mm in diameter, collimated beam. That beam was focused onto the sample surface using a 20mm focal length AR-coated planoconvex lens. This configuration provided lateral resolution of approximately 20mm and an axial resolution of 10mm in air with a dynamic range of 40–50dB. The PS-OCT system is completely controlled using Labview software (National Instruments, Austin, TX). The system is described in greater detail [7,22]. Acquired scans

are compiled into b-scan files. Image processing was carried out using Igor Pro, data analysis software (Wavemetrics Inc., Lake Oswego, OR).

Digital and Polarized Light Microscopy

Images of the bovine blocks were examined using a digital microscopy/3D surface profilometry system, the VHX-1000 from Keyence (Elmwood, NJ) with the VH-Z25 lens with a magnification from 25 to 175x. Images were acquired by scanning the image plane of the microscope and reconstructing a depth composition image with all points at optimum focus displayed in a 2D image.

Serial sections, approximately 200 μm thick were cut using an Isomet 5000 saw (Buehler, IL), for polarized light microscopy (PLM). PLM was carried out using a Meiji Techno RZT microscope (Meiji Techno Co., LTD, Saitama, Japan) with an integrated digital camera, Canon EOS Digital Rebel XT (Canon Inc., Tokyo, Japan). The sample sections were imbibed in water and examined in the brightfield mode with crossed polarizers and a red I plate with 500-nm retardation.

Analysis of Erosion Rates From OCT Scans

Co-polarization OCT scans were used to determine the depths of both the laser treated windows (L) and the central unprotected window (U). The protective varnish was only removed after the final period of erosion (Day 6). Therefore it was only possible to calculate the absolute depths of erosion after removal of the varnish and measurement of the difference in the respective surface positions in the OCT scans between the treatment windows and the protected windows (P) for Day 6 (see Fig. 3). It was possible to monitor the relative difference in the depths of erosion between the (L) and (U) windows (Differential Depth) during the intermediate time points by comparing the difference in the position of the surfaces of the (L) and (U) windows and a line drawn connecting the surfaces of the two sound protected windows (P) with the varnish intact (Fig. 3).

The OCT and PLM depths were compared for the (L) and (U) groups using a *t*-test and the OCT differential depths were compared using repeated measures ANOVA with the Tukey post test. Statistical calculations were carried out using Prism (Graphpad Software, La Jolla, CA).

Analysis of ΔR From OCT Scans

Cross-polarization OCT scans were assessed to evaluate the integrated reflectivity (ΔR) over the depth of demineralization in units of (dB × μm) using a program written in Labview. The program derived two-dimensional projections of the lesion depth and integrated reflectivity [23].

Raw OCT data was linearized and an area of each b-scan outside of the sample was selected to represent the magnitude of the background noise. This value was used to reduce the speckle noise by employing a threshold value (four times the background standard deviation plus the mean background intensity) to ensure with 99.994% certainty that the accepted signal exceeds the noise [20,24]. A Gaussian blur was applied through a convolution matrix

for the elimination of speckle noise, retention of signal peaks and for the selection of integration boundaries. The data set was thresholded a second time, before any depth or integrated reflectivity calculations were performed, to discriminate peaks from sound tissue and that of demineralized enamel. It was empirically determined through analysis of sound samples that demineralized enamel can be identified as having a greater than or equal to 90% contrast for signal amplitude relative to background signal [20,24]. Peaks for which this threshold is not met are considered to be sound.

For the determination of lesion depths and integration boundaries, an edge-detection approach was used which identified the enamel surface and the deep lesion boundary by application of an edge locator. The OCT data was rescaled to range from 0 to the maximum value by subtraction of the minimum noise level. The depth of the demineralization (lesion depth) was calculated by locating the upper and lower lesion boundaries of the lesion signal by identifying the first pixels that fail to meet the requirement of being greater than or equal to Ae^{-2}, where A is the peak maximum. The spatial dimensions per-pixel were obtained experimentally by system calibration and used to convert pixel depths to micrometer depths. In a prior study, reported OCT lesion depths were verified by histological examination of sectioned samples and measurement using PLM [23]. ΔR was calculated by integration of the signal peak within the boundaries of the sample surface and the calculated depth of demineralization (lesion depth). The values reported are in micron × volts/3.2×10^{-5}. The reported ΔR values represent mean values over a 1 mm^2 area centered on each window. The mean ΔR values were compared using two-way repeated measures ANOVA with the Tukey post test. Time of erosion and treatment group (L & U) were the row and column variables.

Since the subsurface demineralization was accompanied by considerable erosion a modified ΔR was also calculated (Mod ΔR) after 6-days of erosion by adding the product of the depth of erosion and the maximum reflectivity near the surface of the lesion. This corrects for the integrated reflectivity of the enamel that was completely lost due to erosion. This approach is analogous to calculating the total mineral loss by adding the product of 80% mineral—sound enamel mineral content— and the depth of erosion to ΔZ, the integrated mineral loss with depth, determined using microradiography [25,26]. The Mod ΔR values were compared using a *t*-test.

RESULTS

There were obvious visual changes in the laser treated and untreated windows after exposure to 6-days of acid challenge. Figures 1 and 2 show depth composition digital microscopy images of the sample windows before and after exposure to the acid challenge. Even though the areas exposed to the acid challenge appeared whiter due to increased light scattering (windows L & U of Fig. 2), one typically could not resolve differences between the laser treated and unprotected windows by visual inspection alone. At high magnification the laser treated surface had a worm-like pattern due to melting (Fig. 1 (L)). Even after exposureto6-days of acid challenge that worm-like pattern was still apparent on many of the laser treated windows showing that much of the surface modified by the laser remained intact (Fig. 2 (L)). A few of the samples showed large variations in the depth of erosion in the unprotected areas as can be seen in Figure 2 (U) but most appeared similar to the laser treated windows

at low magnification. Sequential parallel-axis OCT b-scans were taken at different pH cycling time periods (0, 2, 4, 6 days) and examples for one sample are shown in Figure 3. The goal of our study was to investigate the use of laser-modified enamel surfaces or marks to serve as a reference for the nondestructive assessment of erosion rates *in vivo*. The laser irradiated enamel surfaces manifested little erosion after 6 days of exposure; while the unprotected region of the samples exhibited markedly higher erosion, ~ 100 μm.

Figure 4 shows a matched OCT b-scan along with a PLM image from the same sample. The images are very similar showing the more severe erosion in the central window along with the greater depth of subsurface demineralization.

After the 6-day of pH cycling the acid resistant varnish was removed allowing the direct measurement of the depth of erosion in the central unprotected window and the laser treated windows. The depth of erosion was measured relative to the protected (outer windows) after removal of the varnish. The left and right laser treated windows were averaged for comparison with the central window. The mean eroded depth (±s.d) is shown in Figure 5. During the pH cycling process we had to acquire the OCT scans without removal of the acid resistant varnish. Therefore, it was only possible to measure the depth differential between the central unprotected window and the adjoining laser treated windows. This approach is feasible clinically where only differential depth measurements would be possible. The mean depth differential (±s.d) is shown in Figure 6 for the four time periods. After 6-days the mean depth differential was ~ 70 μm which is quite large and is not far from the actual eroded depth of ~ 90 μm.

In addition to erosion the exposed windows manifested considerable subsurface demineralization. The severity of subsurface demineralization was assessed by calculation of the integrated reflectivity with lesion depth (ΔR, dB × μm) from the cross-polarization OCT images. Since the subsurface demineralization was accompanied by considerable erosion a mod ΔR was also calculated after 6-days of acid challenge by adding the product of the depth of erosion and the reflectivity at the surface of the lesion to the measured ΔR. The mean depths of erosion measured using OCT and PLM, the mean differential depths and the mean values for ΔR and mod ΔR for demineralization are tabulated in Table I.

DISCUSSION

These results suggest that it may be feasible to utilize these laser-irradiated (protected) areas generated with sub-ablative fluence to monitor erosion. Our studies indicated that after 6-days of pH cycling, laser irradiated enamel inhibited erosion by 74%. It is important to note that bovine enamel blocks were employed in these studies which are slightly more susceptible to demineralization and erosion than human enamel and the severity of erosion and demineralization would be expected to be less for human enamel.

A comparison of the mean depths of erosion shown in Table I measured using OCT and PLM indicate markedly higher depths for PLM. During sectioning the fragile areas of subsurface demineralization typically break off. An example of this can be seen in Figure 4. The left laser treated area is mostly intact in the OCT scan (Fig. 4 B) with the exception of a

small depression at the outer edge. However, in the corresponding PLM image (Fig. 4A) the left laser treated area is not intact and there is considerable loss of enamel. The ability to measure the enamel loss without sectioning the samples is a significant advantage of OCT since with PLM it is not clear how much of the enamel is lost in the sectioning process.

Previous studies identified that the layer of modified enamel after irradiation with 9.3 μm CO_2 laser pulses of 10–15 μs duration is only 10–20 μm thick [19]. This study indicates that the laser-irradiated areas underwent a mean loss of 30 μm of enamel which is deeper than the thickness of modified enamel. However, for some of the samples (see Fig. 2) much of the laser treated area remained relatively intact.

There have been many studies on the use of thermal treatments and lasers, including pulsed carbon dioxide lasers operating at 9.3–9.6 μm, to inhibit the demineralization of enamel [17,18,27–32]. However, there have been few studies investigating the use of lasers to inhibit surface loss or erosion [33–35]. Steiner-Oliveira et al. [35] explored the use of a CO_2 laser operating at 10.6 μm with a pulse duration of 5,000 μs with and without topical fluoride for the inhibition of erosion. They did not observe significant inhibition of erosion on bovine enamel by the laser alone. However, they used an incident fluence of only 1J/cm^2, which is unlikely to raise the enamel temperature sufficiently to cause any thermal decomposition or transformation of the enamel. In this study we used a wavelength of 9.3 μm which is more strongly absorbed (μ_a = 5250cm^{-1}) vs. (μ_a = 825cm^{-1}) for 10.6 μm; a magnitude of six times higher [19]. Moreover, the pulse duration employed in our study was 15μs vs. the 5,000 μs pulse duration used in their study. A pulse of 5,000μs is too long and allows heat to flow away from the treated area rendering the heat deposition process highly inefficient. In addition, we deliberately created a melt layer on the enamel surface that was observable (Fig. 1) providing confirmation that the enamel was actually thermally modified.

As mentioned in previous studies, the efficacy of protection against erosion from the laser-modified area depends on the severity of demineralization. The pH cycling model proved to be quite severe in our study, since it eroded roughly 100μm of enamel. We propose that erosion can be monitored *in vivo* by producing two small parallel lines of laser modified enamel on the tooth surface and monitoring the depth differential with the unprotected zone in between. Clinical studies will be needed to establish whether this method will work *in vivo* or *in situ* over a wide range of acid or erosive challenges including the influence of mechanical wear on the laser treated surfaces.

Acknowledgments

This work was supported by NIH/NIDCR Grants R01-DE17869 and R01-DE19631.

References

1. Jaeggi T, Lussi A. Prevalence, incidence and distribution of erosion. Monogr Oral Sci. 2006; 20:44–65. [PubMed: 16687884]
2. Ganss C, Lussi A. Diagnosis of erosive tooth wear. Monogr Oral Sci. 2006; 20:32–43. [PubMed: 16687883]

3. Baumgartner A, Dicht S, Hitzenberger CK, Sattmann H, Robi B, Moritz A, Sperr W, Fercher AF. Polarization-sensitive optical optical coherence tomography of dental structures. Caries Res. 2000; 34:59–69. [PubMed: 10601786]
4. Wang XJ, Zhang JY, Milner TE, Boer JFd, Zhang Y, Pashley DH, Nelson JS. Characterization of Dentin and Enamel by use of Optical Coherence Tomography. Appl Opt. 1999; 38(10):586–590.
5. Everett MJ, Colston BW, Sathyam US, Silva LBD, Fried D, Featherstone JDB. Non-invasive diagnosis of early caries with polarization sensitive optical coherence tomography (PS-OCT). Lasers in Dentistry V Proc Soc Photo Opt Instrum Eng. 1999; 3593:177–183.
6. Feldchtein FI, Gelikonov GV, Gelikonov VM, Iksanov RR, Kuranov RV, Sergeev AM, Gladkova ND, Ourutina MN, Warren JA, Reitze DH. In vivo OCT imaging of hard and soft tissue of the oral cavity. Opt Express. 1998; 3(3):239–251. [PubMed: 19384366]
7. Fried D, Xie J, Shafi S, Featherstone JDB, Breunig T, Lee CQ. Early detection of dental caries and lesion progression with polarization sensitive optical coherence tomography. J Biomed Opt. 2002; 7(4):618–627. [PubMed: 12421130]
8. Jones RS, Fried D. Remineralization of enamel caries can decrease optical reflectivity. J Dent Res. 2006; 85(9):804–808. [PubMed: 16931861]
9. Ngaotheppitak P, Darling CL, Fried D. Polarization optical coherence tomography for measuring the severity of caries lesions. Lasers Surg Med. 2005; 37(1):78–88. [PubMed: 15889402]
10. Lee C, Darling C, Fried D. Polarization sensitive optical coherence tomographic imaging of artificial demineralization on exposed surfaces of tooth roots. Dent Mater. 2009; 25(6):721–728. [PubMed: 19167052]
11. Manesh SK, Darling CL, Fried D. Nondestructive assessment of dentin demineralization using polarization-sensitive optical coherence tomography after exposure to fluoride and laser irradiation. J Biomed Mater Res B Appl Biomater. 2009; 90(2):802–812. [PubMed: 19283826]
12. Manesh SK, Darling CL, Fried D. Polarization-sensitive optical coherence tomography for the nondestructive assessment of the remineralization of dentin. J Biomed Opt. 2009; 14(4):044002. [PubMed: 19725714]
13. Louie T, Lee C, Hsu D, Hirasuna K, Manesh S, Staninec M, Darling CL, Fried D. Clinical assessment of early tooth demineralization using polarization sensitive optical coherence tomography. Lasers Surg Med. 2010; 42(10):738–745. [PubMed: 21246578]
14. Staninec M, Douglas SM, Darling CL, Chan K, Kang H, Lee RC, Fried D. Nondestructive clinical assessment of occlusal caries lesions using near-IR imaging methods. Lasers Surg Med. 2011; 43(10):951–959. [PubMed: 22109697]
15. Wilder-Smith CH, Wilder-Smith P, Kawakami-Wong H, Voronets J, Osann K, Lussi A. Quantification of dental erosions in patients with GERD using optical coherence tomography before and after double-blind, randomized treatment with esomeprazole or placebo. Am J Gastroenterol. 2009; 104(11):2788–2795. [PubMed: 19654570]
16. Chan KH, Chan AC, Darling CL, Fried D. Methods for monitoring erosion using optical coherence tomography. Lasers in Dentistry XIX Proc Soc Photo Opt Instrum Eng. 2014; 8566:1–5.
17. Featherstone JD, Barrett-Vespone NA, Fried D, Kantorowitz Z, Seka W. CO_2 laser inhibitor of artificial caries-like lesion progression in dental enamel. J Dent Res. 1998; 77(6):1397–1403. [PubMed: 9649168]
18. Fried D, Featherstone JD, Le CQ, Fan K. Dissolution studies of bovine dental enamel surfaces modified by high-speed scanning ablation with a λ=93-microm TEA CO_2 laser. Lasers Surg Med. 2006; 38(9):837–845. [PubMed: 17044095]
19. Zuerlein M, Fried D, Featherstone JDB. Modeling the modification depth of carbon dioxide laser treated enamel. Lasers Surg Med. 1999; 25:335–347. [PubMed: 10534750]
20. Le MH, Darling CL, Fried D. Automated analysis of lesion depth and integrated reflectivity in PS-OCT scans of tooth demineralization. Lasers Surg Med. 2010; 42(1):62–68. [PubMed: 20077486]
21. Chan KH, Tom H, Fried D. Monitoring the inhibition of erosion by a CO_2 laser with OCT. Lasers in Dentistry XX Proc Soc Photo Opt Instrum Eng. 2014; 89290:1–5.
22. Bush J, Davis P, Marcus MA. All-fiber optic coherence domain interferometric techniques. Fiber Optic Sensor Technology II Proc Soc Photo Opt Instrum Eng. 2000; 4204:71–80.

23. Chan KH, Chan AC, Fried WA, Simon JC, Darling CL, Fried D. Use of 2D images of depth and integrated reflectivity to represent the severity of demineralization in cross-polarization optical coherence tomography. J Biophotonics. 2013 In Press.
24. Kang H, Jiao JJ, Chulsung L, Le MH, Darling CL, Fried DL. Nondestructive assessment of early tooth demineralization using cross-polarization optical coherence tomography. IEEE J Sel Top Quantum Electron. 2010; 16(4):870–876. [PubMed: 21660217]
25. Arends J, Ruben JL, Inaba D. Major topics in quantitative microradiography of enamel and dentin: R parameter, mineral distribution visualization, and hyper-remineralization. Adv Dent Res. 1997; 11(4):403–414. [PubMed: 9470497]
26. Darling CL, Featherstone JDB, Le CQ, Fried D. An automated digital microradiography system for assessing tooth demineralization. Lasers in Dentistry VX Proc Soc Photo Opt Instrum Eng. 2009; 7162:1–7.
27. Kuroda S, Fowler BO. Compositional, structural and phase changes in *in vitro* laser-irradiated human tooth enamel. Calcif Tissue Int. 1984; 36:361–369. [PubMed: 6435835]
28. Fowler B, Kuroda S. Changes in heated and in laser-irradiated human tooth enamel and their probable effects on solubility. Calcif Tissue Int. 1986; 38:197–208. [PubMed: 3011230]
29. Nelson DGA, Shariati M, Glena R, Shields CP, Featherstone JDB. Effect of pulsed low energy infrared laser irradiation on artificial caries-like lesion formation. Caries Res. 1986; 20:289–299. [PubMed: 3459578]
30. Featherstone JDB, Nelson DGA. Laser effects on dental hard tissue. Adv Dent Res. 1987; 1(1):21–26. [PubMed: 3125842]
31. Fried D, Murray MW, Featherstone JDB, Akrivou M, Dickenson KM, Duhn C. Dental hard tissue modification and removal using sealed TEA lasers operating at λ=96μm. J Biomed Opt. 2001; 6(2):231–238. [PubMed: 11375734]
32. Rechmann P, Fried D, Le CQ, Nelson G, Rapozo-Hilo M, Rechmann BM, Featherstone JD. Caries inhibition in vital teeth using 96μm CO_2 laser irradiation. J Biomed Opt. 2011; 16(7):071405. [PubMed: 21806251]
33. Vlacic J, Meyers IA, Kim J, Walsh LJ. Laser-activated fluoride treatment of enamel against an artificial caries challenge: comparison of five wavelengths. Aust Dent J. 2007; 52(2):101–105. [PubMed: 17687954]
34. Vlacic J, Meyers IA, Walsh LJ. Laser-activated fluoride treatment of enamel as prevention against erosion. Aust Dent J. 2007; 52(3):175–180. [PubMed: 17969284]
35. Steiner-Oliveira C, Nobre-dos-Santos M, Zero DT, Eckert G, Hara AT. Effect of a pulsed CO_2 laser and fluoride on the prevention of enamel and dentine erosion. Arch Oral Biol. 2010; 55(2): 127–133. [PubMed: 20031117]

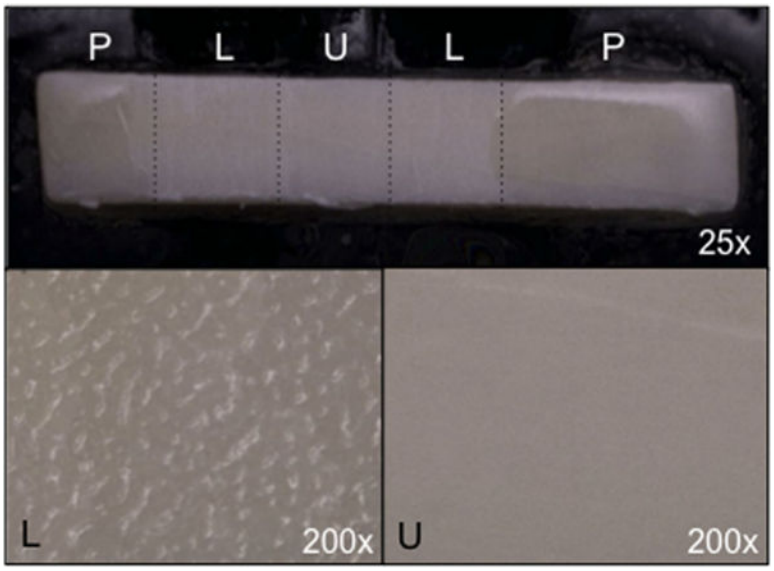

Fig. 1.

Depth composition images of a bovine enamel block with the five treatment windows at (25×) magnification prior to exposure to the erosion solution (0 days). The windows marked (P) were covered with a clear acid resistant varnish, (L) were irradiated by the laser and (U) was unprotected. Higher magnification (200×) images of the (L) and (U) windows are also shown. Note the patterned surface after laser irradation.

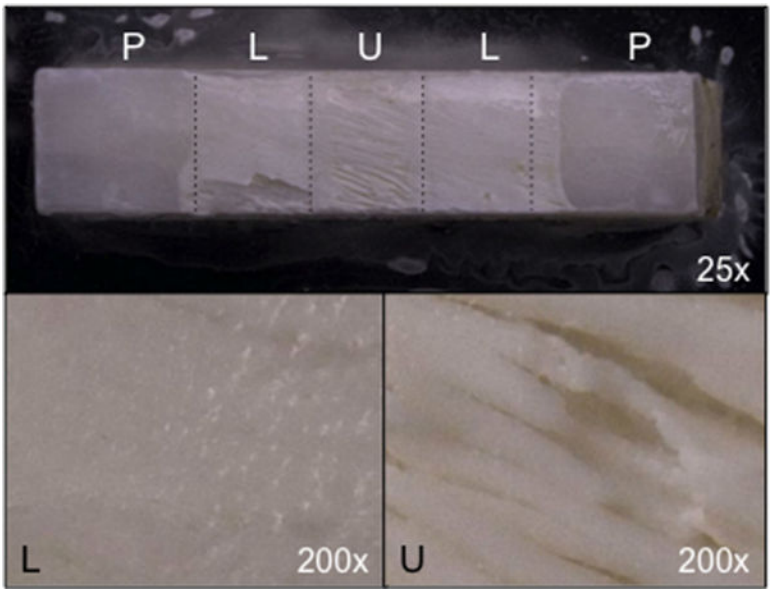

Fig. 2.

Depth composition images of a bovine enamel block with the five treatment windows at (25×) magnification after 6-days of erosion. The windows marked (P) were covered with a clear acid resistant varnish, (L) were irradiated by the laser and (U) was unprotected. Higher magnification(200×) imagesofthe(L) and (U) windows are also shown. Note that some of the original pattern on the enamel surface still remains after 6-days of pH cycling while the unprotected window shows nonuniform erosion.

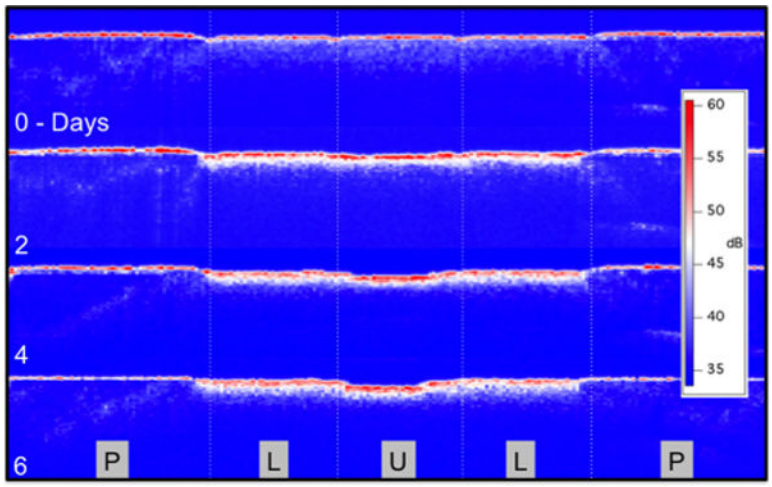

Fig. 3.

Co-polarization OCT b-scans during consecutive pH cycling time periods for one sample. The periods of pH cycling, 0, 2, 4, and 6-days are shown and the different windows: (P) protected, (L) laser and (U) protected are separated by the dotted lines. The increased erosion in the unprotected center window is clearly visible.

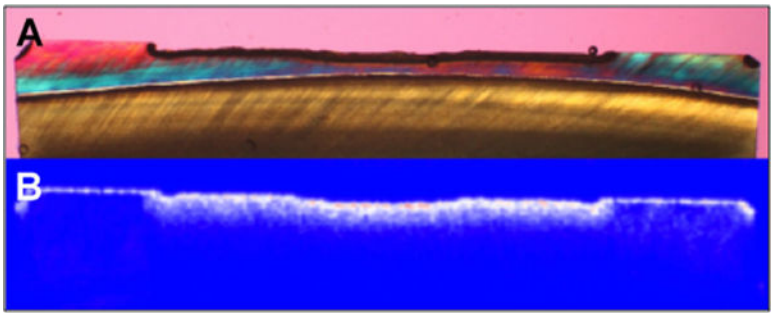

Fig. 4.

A polarized light micrograph of a thin section cut from one of the samples (A) is shown with the matched co-polarization OCT b-scan image (B) after 6-days of erosion.

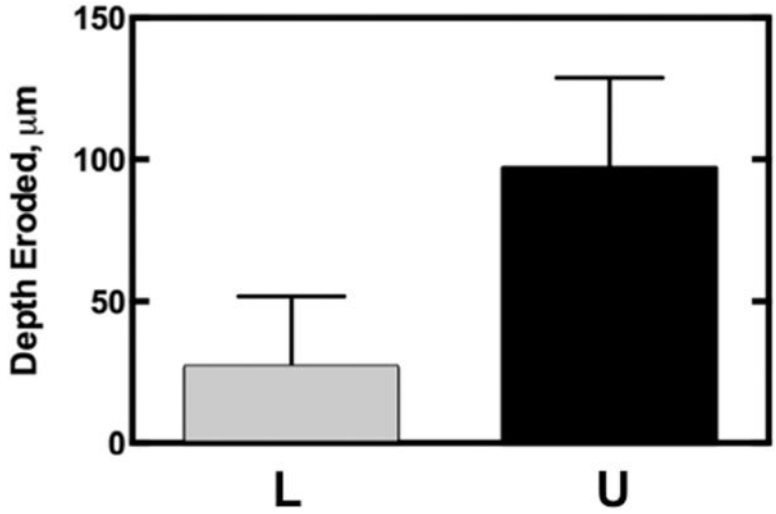

Fig. 5.

The mean depth eroded ± s.d for the laser treated (L) and unprotected (U) groups after 6-days of erosion.

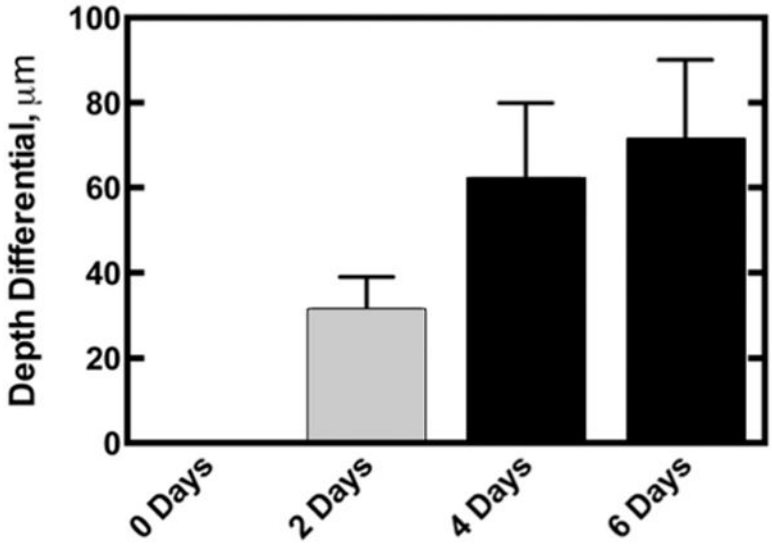

Fig. 6.

The mean depth differential ± s.d between the laser treated and unprotected regions after each day of erosion.

TABLE I

The Mean (± s.d.) Values for the OCT and PLM Measurements. Groups Containing the Same Letter in Each Column are Statistically Similar ($P > 0.05$).

pH Cycles	0	2	4	6
OCT Depth, μm (L)	—	—	—	26 (24)
(U)	—	—	—	91 (39)
PLM Depth, μm (L)	—	—	—	75 (16)
(U)	—	—	—	133 (34)
OCT Diff. Depth, μm	0	31 (8)	63 (19) a	68 (18) a
ΔR, μm × dB (L)	1914 (2276) b	4475 (1355) b	6361 (629)	7287 (715) c
(U)	2360 (2584) b	3969 (873) b	5845 (549)	6993 (613) c
Mod ΔR, μm × dB (L)	—	—	—	8448 (1524)
(U)	—	—	—	11280 (1827)